The LKB1-AMPK-α1 signaling pathway triggers hypoxic pulmonary vasoconstriction downstream of mitochondria

Moral-Sanz, Javier; Lewis, Sophronia A.; MacMillan, Sandy; Ross, Fiona A.; Thomson, Adrian; Viollet, Benoit

Published in:
Science Signaling

DOI:
10.1126/scisignal.aau0296

Publication date:
2018

Document Version
Peer reviewed version

The LKB1-AMPK-α1 signalling pathway triggers hypoxic pulmonary vasoconstriction downstream of mitochondria

Javier Moral-Sanz BSc, PhD[1$], Sophronia A. Lewis BSc, PhD [1$], Sandy MacMillan BSc[1], Fiona A. Ross BSc, PhD [2], Adrian Thomson[3], Benoit Viollet BSc, PhD [4,5,6], Marc Foretz BSc, PhD [4,5,6], Carmel Moran BSc, PhD [3], D. Grahame Hardie BSc, PhD [2], A. Mark Evans BSc, PhD [1*]

[1]Centre for Discovery Brain Sciences and Cardiovascular Science, College of Medicine and Veterinary Medicine, Hugh Robson Building, University of Edinburgh, Edinburgh, EH8 9XD, UK. [2]Division of Cell Signalling & Immunology, School of Life Sciences, University of Dundee, Dow Street, Dundee, DD1 5EH, UK. [3]Centre for Cardiovascular Science, Queen's Medical Research Institute, University of Edinburgh, Edinburgh, EH16 4TJ, UK. [4]Institut Cochin, INSERM U1016, [5]CNRS UMR 8104 and [6]Université Paris Descartes, Sorbonne Paris cité, 75014 Paris, France.

[$]Both authors contributed equally.

Corresponding Author: Professor A. Mark Evans, Centre for Discovery Brain Sciences and Cardiovascular Science, University of Edinburgh, Hugh Robson Building, George Square, Edinburgh EH8 9XD, UK. Tel: +441316511501; Email: mark.evans@ed.ac.uk

Abstract

Hypoxic pulmonary vasoconstriction (HPV), which aids ventilation-perfusion matching in the lungs, is triggered by mechanisms intrinsic to pulmonary arterial smooth muscles. The unique sensitivity of these muscles to hypoxia is conferred by mitochondrial cytochrome c oxidase subunit 4 isoform 2, the inhibition of which has been proposed to trigger HPV through increased generation of mitochondrial reactive oxygen species. Contrary to this model, we have shown that the LKB1-AMPK-α1 signaling pathway is critical to HPV. Here, spectral Doppler-ultrasound revealed that deletion of the AMPK-α1 catalytic subunit blocked HPV in mice during mild (8% O_2) and severe (5% O_2) hypoxia, whereas AMPK-α2 deletion attenuated HPV only during severe hypoxia. By contrast, neither of these genetic manipulations affected serotonin-induced reductions in pulmonary vascular flow. HPV was also attenuated by reduced expression of LKB1, a kinase that activates AMPK during energy stress, but not after deletion of CaMKK2, a kinase that activates AMPK in response to increases in cytoplasmic Ca^{2+}. Fluorescence imaging of acutely isolated pulmonary arterial myocytes revealed that AMPK-α1 or AMPK-α2 deletion did not affect mitochondrial membrane potential during normoxia or hypoxia. However, deletion of AMPK-α1, but not of AMPK-α2, blocked hypoxia from inhibiting $K_V1.5$, the classical "oxygen-sensing" K^+ channel in pulmonary arterial myocytes. We conclude that LKB1-AMPK-α1 signaling pathways downstream of mitochondria are critical for the induction of HPV, in a manner also supported by AMPK-α2 during severe hypoxia.

Hypoxic pulmonary vasoconstriction (HPV) (*1*) diverts blood flow from oxygen-deprived to oxygen-rich areas of the lung, thus matching perfusion with ventilation (*2*). However when triggered by prolonged and widespread hypoxia, such as during ascent to altitude (*3*) or disease (such as cystic fibrosis), HPV can cause hypoxic pulmonary hypertension (HPH) leading to right heart failure (*4*).

HPV is initiated by airway hypoxia rather than by vascular hypoxaemia (*5*), through constriction of pre-capillary resistance arteries by signalling pathways that are intrinsic to their smooth muscle and endothelial cells (*6-8*), and are independent of blood-borne mediators or the autonomic nervous system (*9, 10*). The initiation phase of acute HPV is driven by smooth muscle constriction, which is later augmented by an endothelium-derived vasoconstrictor (*6, 11*). The threshold for HPV is ≈80 mm Hg O_2 (*12*), beyond which the magnitude of HPV increases with the degree of hypoxia. The unique oxygen-sensitivity of pulmonary arterial myocytes is conferred by mitochondrial cytochrome c oxidase subunit 4 isoform 2 (COX4I2), the deletion of which blocks HPV (*13*). HPV has been proposed to be triggered by increases in mitochondrial reactive oxygen species (ROS) upon inhibition of mitochondrial metabolism at the COX-COX4I2 complex (*13*). In this respect, however, it is evident that COX-COX4I2 deletion will not only compromise mitochondrial ROS production during hypoxia, but will also raise the threshold at which hypoxia evokes increases in the cytoplasmic AMP:ATP / ADP:ATP ratios (*13*). This is critical because we previously proposed that HPV is mediated not by ROS but by the AMP-activated protein kinase (AMPK) (*14*). Supporting this notion, small molecule AMPK activators induce pulmonary artery constriction by mechanisms similar to those employed by hypoxia (*14*), and each of these stimuli are mutually exclusive with respect to inhibition of $K_V1.5$ (*15*), the archetypal oxygen-sensing potassium channel in pulmonary arterial myocytes (*8, 16*). That said, ROS have been proposed to activate AMPK directly (*17, 18*), although this view has been controversial (*19, 20*).

AMPK is a cellular energy sensor that occurs as heterotrimeric complexes comprising one catalytic α subunit (α1/α2) in combination with one β (β1/β2) and one γ subunit (γ1/γ2/γ3); these subunit isoforms generate up to 12 different combinations, with different sensitivities to metabolic stress and the capacity to regulate different downstream targets (*21*). In response to metabolic stresses such as hypoxia and mitochondrial poisons, binding of AMP to the γ subunit increases AMPK activity by up to 10-fold through allosteric activation. However, it is the upstream kinase liver kinase B1 (LKB1) that is most critical to AMPK activation under these conditions. LKB1 is thought to be constitutively active (*22, 23*). Upon binding of AMP and/or ADP to the AMPK γ subunit, phosphorylation of Thr^{172} on the α subunit is enhanced, and dephosphorylation of Thr^{172} inhibited, yielding up to a 100-fold increase in AMPK activity through a net increase in phosphorylation of Thr^{172} by LKB1. All three of these effects are blocked by high concentrations of ATP. AMPK activation may also be triggered independently of metabolic stresses, through increases in intracellular Ca^{2+} and increases in Thr^{172} phosphorylation mediated by the calmodulin-dependent kinase, CaMKK2 (*21*). Once activated, AMPK phosphorylates targets that switch off non-essential ATP-consuming processes and switch on catabolic pathways generating ATP, thereby compensating for deficits in ATP supply caused by, for example, inhibition of mitochondrial oxidative phosphorylation.

We sought to determine whether AMPK signalling pathways within pulmonary arterial myocytes initiate HPV downstream of mitochondria, by studying transgenic mice deficient in LKB1, CaMKK2 or AMPK. Our findings show that activation of the LKB1-AMPK-α1 signalling pathway within pulmonary arterial smooth muscles is critical for the initiation of HPV.

Results

We sought to determine the role of AMPK in the induction of HPV, the initiating phase of which is primarily driven by mechanisms of constriction intrinsic to pulmonary arterial myocytes (*6*). The genes encoding the AMPK-α1 (*Prkaa1*) or AMPK-α2 (*Prkaa2*) catalytic subunits were conditionally deleted (Fig. S1), by crossing floxed mice with those expressing Cre recombinase from the *transgelin* promoter. AMPK-α1 and AMPK-α2 knockout mice did not exhibit overt phenotypes, although mild left, but not right, ventricular myopathy was evident after AMPK-α2 deletion alone (Table S1). This finding is consistent with previous reports of a dominant role for AMPK-α2 in the regulation of cardiomyocyte metabolism and growth (*24, 25*).

However, AMPK-α1 or AMPK-α2 deletion attenuated HPV, which was monitored using spectral Doppler ultrasound analysis of systolic peak velocity and velocity time integral (VTI) within the main pulmonary artery. This method provides an index of dynamic changes in pulmonary vascular flow (*26*). Only AMPK-α1 deletion markedly attenuated HPV in mice exposed to both mild (8% O_2; Fig. S2A and S2B) and severe hypoxia (5% O_2; Fig. 1A, 1B, 1C and 1D; Fig. S2A and S2B; Fig. S3A and S3B). Moreover, the magnitude of HPV increased with the severity of hypoxia in floxed, control mice but not in AMPK-α1 knockouts (Fig. 1A; Fig. S2A and S2B). By contrast, AMPK-α2 deletion attenuated HPV evoked by severe (5% O_2; Fig. 1A, 1C and 1D) but not mild (8% O_2) hypoxia (Fig. S2A and S2B; Fig. S3A and S3B). Furthermore, the degree to which HPV was attenuated during severe hypoxia appeared to be slightly more marked for AMPK-α1 than for AMPK-α2 knockouts, although this difference was not significant (Fig. 1D; Fig. S2A and S2B; Fig. S3A and S3B). Collectively, these data suggest that AMPK-α1 may be critical to the induction of HPV, whereas AMPK-α2 supports HPV in some other way during severe hypoxia. In contrast, neither AMPK-α1 nor AMPK-α2 deletion affected increases in pulmonary vascular reactivity induced by intravenous injection of serotonin (Fig. 1E, 1F, 1G and 1H; Fig. S3C and S3D), a

pulmonary-selective vasoconstrictor (*27*) that promotes pulmonary hypertension by different mechanisms to hypoxia (*28*). Moreover, AMPK-α1 and AMPK-α2 deletion inhibited pulmonary vascular responses during hypoxia, but did not affect either resting systemic arterial blood pressures or hypoxia-evoked decreases in systemic arterial blood pressures (*29*). Thus, deletion of AMPK-α1 and AMPK-α2 subunits within arterial myocytes selectively inhibits HPV. This view is supported by the findings of others, which have established that neither AMPK-α1 nor AMPK-α2 deletion impacts normoxic or ischemic contracture of cardiac muscles (*24, 30*), and that there is substantial redundancy of function with respect to the regulation by AMPK-α1 and AMPK-α2 of cardiac metabolism and growth (*24, 25, 31*).

We could not generate viable homozygous deletion of the gene encoding LKB1 (*Stk11*) using the trangelin-Cre promoter, but did assess HPV in a strain of mice bearing homozygous floxed alleles of *Stk11*, which globally exhibit hypomorphic (≈90% reduced) expression of LKB1 (*32*). Spectral Doppler analysis of pulmonary arterial systolic waveforms revealed that HPV was markedly attenuated during exposure of these mice to severe hypoxia (5% O_2; Fig. 1D; Fig. S3A and S3B; Fig. S4A). By contrast, global CaMKK2 deletion did not affect hypoxia-evoked reductions in peak velocity (Fig. 1D; Fig. S3A and S3B; Fig. S4B). Therefore, HPV is mediated by LKB1-AMPK signaling independently of the Ca^{2+}/CaMKK2 pathway. Supporting this view, a previous study using the hypomorphic LKB1 model used here has shown that LKB1 deficiency compromises cardiac metabolism but not cardiac contractility, ischemic contracture or recovery from ischemia (*33*).

In isolated pulmonary arterial myocytes, mitochondrial membrane potentials were not affected following deletion of either AMPK-α1 or AMPK-α2 (Fig. 2A and 2B). These gene deletions also did not affect mitochondrial membrane hyperpolarization evoked by hypoxia or oligomycin, which was of similar magnitude to that observed by others (*13*) (Fig. 2C, 2D, 2E and 2F). Consequently,

hypoxia will increase AMP:ATP ratios in pulmonary arterial myocytes (*14*), that will in turn lead to rapid AMPK activation (1-2 min) (*34*). Consistent with this scenario and a requirement for AMPK, AMPK-α1 deletion in acutely isolated pulmonary arterial myocytes attenuated K_V1.5 current inhibition in response to severe hypoxia (≈6% pO_2) (Fig. 3A, 3B, 3C, 3D, 3E, 3F and 3G; Fig. S5A, S5B and S5C), oligomycin and the AMPK-α1 selective activator C13 (*35*) (Fig. 3G). These effects were not due to baseline changes in K_V current amplitudes or kinetics (Table S2). AMPK-α2 deletion did not affect K_V1.5 current inhibition during hypoxia (Fig. 3C, 3F and 3G), supporting the view that AMPK-α1 and not AMPK-α2 drives HPV. The presence of K_V1.5 currents was confirmed using the selective K_V1.5 channel blocker DPO-1 (Fig. 3G and Fig. S6A, S6B, S6C, S6D, S6E and S6F). Therefore, with respect to K_V1.5 current regulation there is no redundancy in the system. Support for this view is provided by the fact that while AMPK-α1 blocked K_V1.5 inhibition during hypoxia, AMPK-α2 deletion did not even affect the time course of K_V1.5 inhibition (Fig. S7A, S7B, S7C and S7D), the onset of which was evident at 1 min and reached a maximum between 2-5min of hypoxia. However, the true time course for K_V1.5 inhibition during hypoxia will likely be faster because the time for complete superfusate exchange and equilibration within the experimental chamber was ≈3-5 min (Fig. S7A, S7B, S7C and S7D). Thus, during hypoxia AMPK-α1 but not AMPK-α2 mediates reductions in K_V1.5 channel activity in pulmonary arterial myocytes during hypoxia, downstream of mitochondrial inhibition.

In contrast to the apparent selectivity of K_V1.5 regulation by endogenous AMPK-α1 in mouse pulmonary arterial myocytes, we have previously shown that exogenous application of recombinant heterotrimers comprising either AMPK-α1 or AMPK-α2 can phosphorylate and regulate K_V1.5 in rat pulmonary arterial myocytes and human K_V1.5 expressed in HEK293 cells (*15*). We have now confirmed sequences surrounding Ser^{559} and Ser^{592} of the human K_V1.5 alpha

subunit (Fig. 4A) as reasonable fits to the AMPK recognition motif using SCANSITE4, as well as an algorithm available on GitHub (https://github.com/BrunetLabAMPK/AMPK_motif_analyzer) (*37, 38*). These motifs lack the expected hydrophobic residue at position P-5, although Ser^{592} does have a large uncharged side chain (Asn) at this position. To identify the AMPK recognition sites that were phosphorylated, we treated the α subunit of the channel from transfected HEK293 cells with protein phosphatase to remove endogenous phosphate groups, before incubating immunoprecipitates with bacterially expressed AMPK (α2β2γ1 complex) (*36*). The stoichiometry of phosphorylation using [γ-^{32}P]ATP was estimated to be 3 moles/mole for wild-type K_V1.5, indicative of multiple sites of phosphorylation (Fig. 4B and 4C). Moreover, the stoichiometry of phosphorylation was reduced on mutating Ser^{559} (2.1 moles/mole) or Ser^{592} (1.2 moles/mole) to alanine, whereas mutation of both sites had a similar effect to mutating Ser^{592} alone, which was also reflected in the average fold change in phosphorylation relative to wild-type with S559A, S592A and S559A/S592A (Fig. 4A, 4B, 4C and 4D). Thus, AMPK directly phosphorylates the α subunit of K_V1.5 at Ser^{592}, and to a lesser extent at Ser^{559}. To assess the role of these sites in K_V1.5 regulation by AMPK, we examined the effect of the AMPK-α1 selective agonist C13 on HEK-293 cells transiently expressing wild-type Kv1.5 α subunit and Kv1.5 α subunits incorporating these single and double mutations. C13 inhibited steady-state currents carried by wild type human K_V1.5 α subunits (Fig. 4E and 4F). This inhibition was virtually abolished by the S559A/S592A double mutation (Fig. 4E, 4F and 4G) and by the S559A mutation (Fig. 4G), and to a lesser extent by the S592A single mutation (Fig. 4G). In short, Ser^{559} phosphorylation confers similar K_V1.5 current inhibition as the S559A/S592A double mutation whereas S592A is less effective, despite the greater effect of the S592A mutation on channel phosphorylation than the S559A mutation.

Discussion

The present investigation showed that divergent LKB1-AMPK signalling pathways coordinated HPV downstream of mitochondria. HPV was suppressed by deletion of either AMPK-α1 or AMPK-α2, whereas reductions in $K_V1.5$ channel activity in pulmonary arterial myocytes during hypoxia were blocked by deletion of AMPK-α1 alone. Furthermore, only AMPK-α1 deletion in smooth muscles blocked the induction and progressive augmentation of HPV by mild and severe hypoxia. By contrast, AMPK-α2 deletion attenuated HPV only during severe hypoxia, indicative of a role for AMPK-α2 containing heterotrimers in supporting HPV during severe hypoxic stress. Outcomes are therefore consistent with our previous studies using the non-selective AMPK antagonist compound C (*39*), although any action of this agent should be considered with caution because compound C inhibits at least ten other kinases more potently than AMPK (*40*). Nevertheless, it is notable that in isolated rat pulmonary artery rings two phases of constriction are evident during hypoxia, both of which are initiated concomitantly and are thus superimposed on each other (*12*). Phases 1 and 2 of HPV are attenuated in pulmonary arteries pre-incubated with compound C, although only the attenuation of Phase 2 is statistically significant (*39*). However, it is open to debate whether the Phase 1 constriction represents a component of the true physiological response of pulmonary arteries in-situ in the lung, given that HPV in the rat lung is abolished by agents that inhibit Phase 2 but not Phase 1 of HPV in acutely isolated pulmonary arteries (*12*).

Although the mode of action by which AMPK-α2 complexes support HPV remains unclear, there is no redundancy of function with respect to either the induction by AMPK-α1 of myocyte contraction during hypoxia or the inhibition of $K_V1.5$. This lack of redundancy is surprising because intracellular dialysis of AMPK heterotrimers containing either AMPK-α1 or AMPK-α2 inhibit $K_V1.5$ in rat pulmonary arterial myocytes (*15*). This suggests that subcellular location rather

than intrinsic target specificity must determine outcomes, with AMPK-α1 complexes in some way "tethered" proximal to the $K_V1.5$ α subunit. Unfortunately, AMPK antibodies that are currently available are not sufficiently specific to directly test this idea. Although we cannot be certain that AMPK phosphorylates $K_V1.5$ directly in hypoxic pulmonary arterial myocytes, given that $K_V1.5$ has been reported to be regulated through tyrosine phosphorylation (*41, 42*), our data do show that AMPK phosphorylates and regulates $K_V1.5$ through serine not tyrosine residues. In short, while multiple kinase pathways may impact $K_V1.5$ activities in pulmonary arterial myocytes, the AMPK-dependent pathway is critical to HPV.

The induction of HPV requires LKB1 but is triggered independently of the Ca^{2+}/CaMKK2 pathway, highlighting that AMPK activation occurs in response to energy stress rather than changes in cytoplasmic Ca^{2+}. This finding suggests that hypoxia-evoked increases in AMP:ATP/ ADP:ATP ratios (*14, 19, 20*) are critical to the process of AMPK activation by hypoxia in pulmonary arterial myocytes. Although a requirement for LKB1 does not rule out a role for mitochondrial ROS in HPV (*13, 17, 18*), it provides further support for the view that mitochondrial ROS do not activate AMPK directly, although ROS may do so indirectly by inhibiting mitochondrial oxidative phosphorylation (*17, 18*). In this context, the possibility that ROS-dependent increases in cytoplasmic Ca^{2+} concentration might contribute to AMPK activation (*43*) seems more remote, given that CaMKK2 is not required for HPV.

It would appear, therefore, that the induction of HPV is primarily governed by the following factors. First, Cox4I2 is selectively expressed in pulmonary arterial smooth muscles, which unlike COX4I1, does not confer COX inhibition by ATP (*44, 45*), such that the rate of oxygen consumption and thus ATP supply through mitochondrial oxidative phosphorylation will not increase during hypoxia as ATP levels fall (*45-48*). Expression of AMPK subunits, particularly

that of AMPK-α1, is higher in pulmonary than in systemic arterial smooth muscles (*14*). Moreover, our data also highlight the potential for the regulation of different targets by divergent AMPK signaling pathways, in a manner that may be facilitated by the selective expression and subcellular targeting of multiple heterotrimeric AMPK subunit combinations.

Thus, our observations implicate AMPK activation as the primary mediator of acute hypoxic pulmonary hypertension consequent to widespread airway hypoxia, an idea consistent with the effects of siRNA knockdown of AMPK in cultured pulmonary arterial myocytes and pharmacological interventions in-vivo (*49*). Moreover, arterial myocyte proliferation during hypoxia and thus hypoxic pulmonary hypertension has been suggested to result from the coordinate regulation by AMPK-α1 and AMPK-α2 of autophagy initiation and inhibition of apoptosis, respectively (*49*). Paradoxically, however, others have proposed that mTORC2-dependent reductions in total AMPK may facilitate myocyte proliferation and thus hypoxic- and idiopathic-pulmonary hypertension through mTORC1 activation (*50*), in a manner that may be exacerbated by endothelial AMPK insufficiency (*51*). One possible explanation for these contrary findings could be that the progression of pulmonary hypertension is governed by temporal fluctuations in AMPK activity and/or expression, a scenario that will require further studies for validation.

The present investigation shows that LKB1-AMPK signalling pathways mediate HPV subsequent to the inhibition of oxidative phosphorylation during hypoxia (*13*), through the phosphorylation and regulation of targets, such as $K_V1.5$, outside of those canonical pathways by which AMPK coordinates cell-autonomous metabolic homeostasis. Therefore, excess AMPK activity or expression may predispose individuals to increases in pulmonary vascular perfusion pressure at high altitudes, and may contribute to the initiation, as well as the progression, of hypoxic pulmonary hypertension (*52*).

Materials and Methods

Mice

Experiments were performed in accordance with the regulations of the United Kingdom Animals (Scientific Procedures) Act of 1986. All studies and breeding were approved by the University of Edinburgh and performed under UK Home Office project licenses. Both male and female mice were used, and all were on a C57/Bl6 background. Numbers of mice (≥ 3 per measure) used are indicated for each experiment.

Gene deletion

Global, dual knockout of the genes encoding AMPK-α1 (*Prkaa1*) and AMPK-α2 (*Prkaa2*) is embryonic lethal. We therefore employed conditional deletion of the genes for the AMPK-α1 or AMPK-α2 subunits, using mice in which the sequence encoding the catalytic site of either or both of the α subunits was flanked by loxP sequences (*53*). To direct AMPK deletion to cells of the smooth muscle lineage, these were crossed with mice in which Cre recombinase was under the control of the transgelin (smooth muscle protein 22α) promoter (The Jackson Laboratory, Bar Harbor, ME, USA [stock number 017491, Tg(Tagln-cre)1Her/J in C57BL/6:129SJL background]). These transgelin-Cre mice do not exhibit Cre expression in endothelial cells, and therefore provide for selective gene deletion in smooth muscle. It should be noted, however, that transient developmental expression of transgelin has been observed in atrial and ventricular myocytes. Therefore, genomic recombination will also occur in these cells although they do not express transgelin in the adult (*54*). However neither atrial nor ventricular myocytes contribute directly or indirectly to acute hypoxic pulmonary vasoconstriction. Therefore, while imperfect, the use of transgelin-Cre mice provided us with the necessary level of specificity to determine the role of AMPK in the response to hypoxia of pulmonary arterial myocytes.

We detected the presence of wild-type or floxed alleles and CRE recombinase by PCR. 10 µl samples were run on 2% agarose gels with 12.5 µl GoTag Green Master Mix M712B (Promega) in TBE buffer against a 100 bp DNA ladder (GeneRuler^{TM}, Fermentas) using a Model 200/2.0 Power Supply (Bio-Rad). Gels were imaged using a Genius Bio Imaging System and GeneSnap software (Syngene). We used four primers for Cre (Transgene 5' GCGGTCTGGCAGTAAAAACTATC 3'and 5' GTGAAACAGCATTGCTGTCACTT 3'; internal positive control 5' CTAGGCCACAGAATTGAAAGATCT 3' and 5' GTAGGTGGAATTTCTAGCATCATCC 3'; expected size for WT=324 bp, expected size for Cre=100 bp). Two primers were used for each AMPK catalytic subunit: α1-forward 5' TATTGCTGCCATTAGGCTAC 3', α1-reverse: 5' GACCTGACAGAATAGGATATGCCCAACCTC 3' (WT=588bp, Floxed=682bp); α2-forward 5' GCTTAGCACGTTACCCTGGATGG 3', α2-reverse: 5' GTTATCAGCCCAACTAATTACAC 3' (WT=204 bp, Floxed=250 bp).

The presence of a wild-type or floxed *Stk11* allele, which encodes for LKB1, was detected using two primers, p200, 5'-CCAGCCTTCTGACTCTCAGG-3' and p201, 5'-GTAGGTATTCCAGGCCGTCA-3'. Deletion of LKB1 in smooth muscle proved to be embryonic lethal. Therefore we studied homozygous LKB1 floxed ($STK11^{flx/flx}$) mice, which are hypomorphic for *LKB1* in all cell types and exhibit ≥90% lower LKB1 expression than $LKB1^{+/+}$ littermates (*32*). To genotype CaMKK2 WT and CaMKK2 knockouts, the presence of a wild-type allele was detected using two primers, KKBeta1, 5' CAGCACTCAGCTCCAATCAA3', and KKBeta2, 5' GCCACCTATTGCC TTGTTTG3', to generate an expected band of 347bp. To detect *CaMKKβ* knockout, a KK2-1 primer was used with KK2-3, 5' TAAGCACAAGCAC TCATTCC3, to generate an expected band of 470bp.

The PCR protocol used for all genotype primers was: 92ºC for 5min, 92ºC for 45s, 56ºC for 45sec, 72ºC for 60s, and 72ºC for 7min for 35 cycles and then 4ºC as the holding temperature.

RNA from control tissues (lung) and arterial smooth muscle was extracted using the High Pure RNA Tissue Kit (Roche) following the manufacturer's guidelines, and the concentration determined using the Nanodrop 1000 spectrophotometer (ThermoScientific). Thereafter cDNA synthesis was carried out using the Transcriptor High Fidelity cDNA synthesis Kit (Roche) following the manufacturers' instructions.

Smooth muscle cell isolation

Adult mice (2-6 months of age) were sacrificed by cervical dislocation. The heart and lungs were removed en bloc and placed in physiological salt solution (PSS) of the following composition NaCl 135, KCl 5, $MgCl_2$ 1, $CaCl_2$ 1, glucose 10, HEPES 10 (pH 7.4). Single smooth muscle cells were isolated from 2^{nd}-3^{rd} order branches of the main intrapulmonary artery. For cell isolation, endothelium denuded arteries were transferred into a nominally calcium free PSS containing (in mg/mL): 1 papain (Sigma), 0.8 Dithio-DL-threitol (Sigma) and 0.7 bovine serum albumin (Sigma) and pre-incubated at 37ºC for 6 min. The tissue was then washed three times in cold PSS without enzymes, and single smooth muscle cells isolated by gentle trituration with a fire-polished Pasteur pipette. Cells were stored in suspension at 4ºC until required.

PCR analysis

2 µl of cDNA in RNase free water was made up to 20 µl with FastStart Universal SYBR Green Master (ROX, 10 µl, Roche), Ultra Pure Water (6.4 µl, SIGMA) and forward and reverse primers for AMPK-α1 and -α2. The sample was then centrifuged and 20 µl added to a MicroAmp™ Fast Optical 96-Well Reaction Plate (Greiner bio-one), the reaction plate sealed with an optical adhesive cover (Applied Biosystems) and the plate centrifuged. The reaction was then run on a sequence detection system (Applied Biosystems) using AmpliTaq Fast DNA Polymerase, with a 2min initial

step at 50°C, followed by a 10min step at 95°C, then 40x 15s steps at 95°C. This was followed by a dissociation stage with 15s at 95°C, 20s at 60°C and 15s at 95°C. Negative controls included control cell aspirants for which no reverse transcriptase was added, and aspiration of extracellular medium and PCR controls. None of the controls produced any detectable amplicon, ruling out genomic or other contamination.

Ultrasound measurements

Mice were rendered anaesthetised using Isoflurane, induced at level 5 and set to level 2 for procedures. Isoflurane was mixed with 21% O_2 set at 1L/min for normoxia and either 12%, 8% or 5% O_2 for the hypoxic challenge (0.05% CO_2, balanced with N_2). Using the Vevo770 (Visualsonics Inc), RMV 707B transducer with a centre frequency of 30MHz, a Parasternal Long Axis (PLAX) view of the heart of anaesthetised mice was obtained, and then modified to bring the pulmonary artery into view for spectral wave Doppler measurements. Peak velocity (mm/s) and velocity time integral (VTI) of pulmonary arterial flow were used as a non-invasive approximation of changes in systolic pulmonary vascular resistance and pressure as described by others(*26*), and this was confirmed here by infusion of a pulmonary selective vasoconstrictor, serotonin, which was applied by intravenously through the tail vein(*27, 52*). Measurement of spectral Doppler velocities were taken under normoxia (21% O_2; 0.05% CO_2 balanced with N_2) and during an acute hypoxic challenge (12%, 8% or 5% O_2; 0.05% CO_2 balanced with N_2) of approximately ~2-5 minutes duration followed by a return to normoxia.

Due to the base-to-apex contraction of the right ventricle (RV), it is difficult to accurately quantify RV function other than by fractional shortening, which was therefore assessed using a two dimensional echocardiographic measurement(*55, 56*). An M-mode across the anterior and posterior left ventricle walls was used to determine fractional shortening of the left ventricle from a standard

PLAX view. To determine RV fractional shortening an M-mode was analysed using ultrasound taken across the right ventricle free wall and the septum from a modified PLAX view(*57*).

Mitochondrial imaging and mitochondrial membrane potential

Fluorescence microscopy was used together with 100 nmol/L Mitotracker Green (490 nm excitation; 516 nm emission) and 100 nmol/L TMRE (Tetramethylrhodamine, ethyl ester; 549 nm excitation; 575 nm emission) or 10 µg/ml Rhodamine 123 (507 nm excitation; 529 nm emission); cells were incubated in PSS each at 37ºC for 30 minutes. Whole-cell Rhodamine 123 fluorescence was analysed before (baseline) and under specified conditions for a maximum of 15 minutes. Non-quenching conditions were confirmed at the end of every experiment by adding the mitochondrial uncoupler carbonyl cyanide 4-(trifluoromethoxy) phenylhydrazone (FCCP; 10 µmol/L). Images of the emitted fluorescence were acquired at 37ºC and 0.1 Hz, using a Zeiss Axiovert 200 with a Zeiss Plan-Apochromat 63x 1.4 n.a.oil immersion objective for TMRE/ Mitotracker Green or with Zeiss Fluar 40x 1.3 n.a oil immersion objective for Rhodamine 123. The microscope was coupled to a Hamamatsu Orca CCD camera and Sutter DG5 light source with appropriate filter sets. Analysis was completed using Volocity 5.5.1 image acquisition and analysis software.

Electrophysiology

K^+ currents were recorded by whole-cell patch clamp and assessed using voltage ramps (-60mV to +60mV; HEK 293 cells) and single (-60 to +50mV; HEK293 cells) or multiple (-80 to +0mV, 10mV increments; pulmonary arterial myocytes) voltage steps. Recordings were conducted at 37°C. The standard perfusate (pH 7.4) was composed of (mM): NaCl 135, KCl 5, $MgCl_2$ 1, $CaCl_2$ 1, glucose 10, HEPES 10 (pH 7.4). Patch pipettes had resistances 4-6 MΩ. Series resistance was monitored and compensated (60-80%) after achieving the whole-cell configuration. If a greater than 20% increase occurred during the recording, the experiment was terminated. The pipette solution (pH 7.2) consisted of (mM): KCl 140; EGTA 10; $MgCl_2$ 1; HEPES 10; Na_2ATP 4,

Na_3GTP 0.1. Cells were normally superfused at a rate of 1 mL/min when drug treatments were tested. To test the effects of hypoxia, cells were superfused at 3 mL/min with bath solution steadily bubbled with 95% N_2 / 5% CO_2 (hypoxia = 6.2 ± 0.3% O_2 in the experimental chamber; as measured with an optical oxygen meter (FireStingO2, PyroScience). All experiments on pulmonary arterial myocyte potassium currents were recorded in the presence of paxilline (1 µmol/L) to block the large conductance voltage- and calcium-activated K^+ channel. Signals were sampled at 10 kHz and low pass filtered at 2 kHz. Conductance values (G) were calculated from the equation G = I/(V − EK), where the Nernst equilibrium potential (EK) was calculated as −89 mV at 37 °C. Normalized conductance/voltage profiles for K_v currents were fitted to a single Boltzmann function with the form $G = G_{max}/(1 + \exp[-(V - V_{0.5})/k])$, where G_{max} is the maximal conductance, $V_{0.5}$ is the test potential for half-maximal conductance ($G_{0.5}$), and k represents the slope of the activation curve. Data are expressed as $I/I_{,max}$, where I_{max} is the current magnitude recorded at the onset of a given experimental intervention. Voltage-clamp acquisition and analysis protocols were performed using an Axopatch 200A amplifier/Digidata 1200 interface controlled by Clampex 10.0 software (Molecular Devices, Foster City, CA). Offline analysis was performed using Clampfit 10.0 (Molecular Devices, Foster City, CA).

HEK 293 cell transfection

HEK 293 cells were cultured in Dulbecco's modified Eagle's medium (DMEM) supplemented with 10% (v/v) fetal bovine serum and 1% (v/v) penicillin/streptomycin. Cells were transfected with 4µg of pcDNA3.1 encoding a wild type or mutant human Kv1.5 (KCNA5) using 10 µL of Lipofectamine 2000 (Thermo Fisher Scientific, Waltham, MA, USA) and used 24-48h later.

Phosphorylation assays

AMPK recognition motifs were identified by medium stringency screen on SCANSITE4 (https://scansite4.mit.edu/4.0/#home), then confirmed and scored on Github

(https://github.com/BrunetLabAMPK/AMPK_motif_analyzer), as previously described by others (*38*). We performed phosphorylation assays using AMPK purified from bacteria and phosphorylated with CaMKK2 (10 units/mL) in the presence of 200μmol/L AMP for 30 min at 30 °C, as described previously (*36*).

Statistical comparisons

Mean ± SEM were compared using GraphPad Prism 6 and: T-test for paired observations; One-way ANOVA with Dunnet or Bonferroni post hoc analysis for multiple comparison's tests. P values < 0.05 were considered significant, assuming mice of a given genotype or cells thereof do not differ in their mean phenotype.

Supplementary Materials

Fig. S1. End-point RT-PCR confirms AMPK deletion.

Fig. S2. AMPK-α1 deletion blocks HPV during moderate and severe hypoxia.

Fig. S3. Effect of deletion of LKB1, AMPK-α1, or AMPK-α2 on peak velocity and velocity time integral.

Fig. S4. HPV requires LKB1 but not CaMKK2.

Fig. S5 Deletion of AMPK-α1 but not AMPK-α2 blocks $K_V1.5$ current inhibition by hypoxia.

Fig. S6. Deletion of AMPK-α1 blocks $K_V1.5$ current inhibition by hypoxia.

Fig. S7 Deletion of AMPK-α1 but not AMPK-α2 blocks $K_V1.5$ current inhibition by hypoxia.

Table S1 Basal cardiolpulmonary hemodynamics.

Table S2 Electrophysiological characteristics of K_V currents.

References and Notes

1. J. R. Bradford, H. P. Dean, The Pulmonary Circulation. *J Physiol* **16**, 34-158 125 (1894).
2. U. S. von Euler, G. Liljestrand, Observations on the pulmonary arterial blood pressure in the cat. *Acta Physiologica Scandinavica* **12**, 301-320 (1946).
3. P. Bartsch, H. Mairbaurl, M. Maggiorini, E. R. Swenson, Physiological aspects of high-altitude pulmonary edema. *J Appl Physiol (1985)* **98**, 1101-1110 (2005).
4. N. Galie, M. M. Hoeper, M. Humbert, A. Torbicki, J. L. Vachiery, J. A. Barbera, M. Beghetti, P. Corris, S. Gaine, J. S. Gibbs, M. A. Gomez-Sanchez, G. Jondeau, W. Klepetko, C. Opitz, A. Peacock, L. Rubin, M. Zellweger, G. Simonneau, Guidelines for the diagnosis and treatment of pulmonary hypertension: the Task Force for the Diagnosis and Treatment of Pulmonary Hypertension of the European Society of Cardiology (ESC) and the European Respiratory Society (ERS), endorsed by the International Society of Heart and Lung Transplantation (ISHLT). *Eur Heart J* **30**, 2493-2537 (2009).
5. E. H. Bergofsky, F. Haas, R. Porcelli, Determination of the sensitive vascular sites from which hypoxia and hypercapnia elicit rises in pulmonary arterial pressure. *Federation Proceedings* **27**, 1420-1425 (1968).
6. M. Dipp, P. C. Nye, A. M. Evans, Hypoxic release of calcium from the sarcoplasmic reticulum of pulmonary artery smooth muscle. *Am J Physiol* **281**, L318-325 (2001).
7. T. P. Robertson, P. I. Aaronson, J. P. Ward, Hypoxic vasoconstriction and intracellular Ca^{2+} in pulmonary arteries: evidence for PKC-independent Ca^{2+} sensitization. *Am J Physiol* **268**, H301-307 (1995).
8. J. M. Post, J. R. Hume, S. L. Archer, E. K. Weir, Direct role for potassium channel inhibition in hypoxic pulmonary vasoconstriction. *Am J Physiol* **262**, C882-890 (1992).
9. R. Naeije, P. Lejeune, M. Leeman, C. Melot, J. Closset, Pulmonary vascular responses to surgical chemodenervation and chemical sympathectomy in dogs. *J Appl Physiol (1985)* **66**, 42-50 (1989); published online EpubJan (
10. E. D. Robin, J. Theodore, C. M. Burke, S. N. Oesterle, M. B. Fowler, S. W. Jamieson, J. C. Baldwin, A. J. Morris, S. A. Hunt, A. Vankessel, et al., Hypoxic pulmonary vasoconstriction persists in the human transplanted lung. *Clinical Sci* **72**, 283-287 (1987).
11. T. P. Robertson, J. P. Ward, P. I. Aaronson, Hypoxia induces the release of a pulmonary-selective, Ca(2+)-sensitising, vasoconstrictor from the perfused rat lung. *Cardiovasc Res* **50**, 145-150 (2001).
12. M. Dipp, A. M. Evans, Cyclic ADP-ribose is the primary trigger for hypoxic pulmonary vasoconstriction in the rat lung in situ. *Circ Res* **89**, 77-83 (2001).
13. N. Sommer, M. Huttemann, O. Pak, S. Scheibe, F. Knoepp, C. Sinkler, M. Malczyk, M. Gierhardt, A. Esfandiary, S. Kraut, F. Jonas, C. Veith, S. Aras, A. Sydykov, N. Alebrahimdehkordi, K. Giehl, M. Hecker, R. P. Brandes, W. Seeger, F. Grimminger, H. A. Ghofrani, R. T. Schermuly, L. I. Grossman, N. Weissmann, Mitochondrial Complex IV Subunit 4 Isoform 2 Is Essential for Acute Pulmonary Oxygen Sensing. *Circ Res* **121**, 424-438 (2017).
14. A. M. Evans, K. J. Mustard, C. N. Wyatt, C. Peers, M. Dipp, P. Kumar, N. P. Kinnear, D. G. Hardie, Does AMP-activated protein kinase couple inhibition of mitochondrial oxidative phosphorylation by hypoxia to calcium signaling in O_2-sensing cells? *J Biol Chem* **280**, 41504-41511 (2005).

15. J. Moral-Sanz, A. D. Mahmoud, F. A. Ross, J. Eldstrom, D. Fedida, D. G. Hardie, A. M. Evans, AMP-activated protein kinase inhibits Kv 1.5 channel currents of pulmonary arterial myocytes in response to hypoxia and inhibition of mitochondrial oxidative phosphorylation. *J Physiol* **594**, 4901-4915 (2016).
16. X. J. Yuan, J. Wang, M. Juhaszova, V. A. Golovina, L. J. Rubin, Molecular basis and function of voltage-gated K^+ channels in pulmonary arterial smooth muscle cells. *Am J Physiol* **274**, L621-635 (1998).
17. B. M. Emerling, F. Weinberg, C. Snyder, Z. Burgess, G. M. Mutlu, B. Viollet, G. R. Budinger, N. S. Chandel, Hypoxic activation of AMPK is dependent on mitochondrial ROS but independent of an increase in AMP/ATP ratio. *Free Radic Biol Med* **46**, 1386-1391 (2009).
18. R. C. Rabinovitch, B. Samborska, B. Faubert, E. H. Ma, S. P. Gravel, S. Andrzejewski, T. C. Raissi, A. Pause, J. St-Pierre, R. G. Jones, AMPK Maintains Cellular Metabolic Homeostasis through Regulation of Mitochondrial Reactive Oxygen Species. *Cell Rep* **21**, 1-9 (2017).
19. G. J. Gowans, S. A. Hawley, F. A. Ross, D. G. Hardie, AMP is a true physiological regulator of AMP-activated protein kinase by both allosteric activation and enhancing net phosphorylation. *Cell Metab* **18**, 556-566 (2013).
20. F. R. Auciello, F. A. Ross, N. Ikematsu, D. G. Hardie, Oxidative stress activates AMPK in cultured cells primarily by increasing cellular AMP and/or ADP. *FEBS Lett* **588**, 3361-3366 (2014).
21. F. A. Ross, C. MacKintosh, D. G. Hardie, AMP-activated protein kinase: a cellular energy sensor that comes in 12 flavours. *FEBS J* **283**, 2987-3001 (2016).
22. G. P. Sapkota, J. Boudeau, M. Deak, A. Kieloch, N. Morrice, D. R. Alessi, Identification and characterization of four novel phosphorylation sites (Ser31, Ser325, Thr336 and Thr366) on LKB1/STK11, the protein kinase mutated in Peutz-Jeghers cancer syndrome. *Biochem J* **362**, 481-490 (2002).
23. K. Sakamoto, O. Goransson, D. G. Hardie, D. R. Alessi, Activity of LKB1 and AMPK-related kinases in skeletal muscle: effects of contraction, phenformin, and AICAR. *Am J Physiol* **287**, E310-317 (2004).
24. E. Zarrinpashneh, K. Carjaval, C. Beauloye, A. Ginion, P. Mateo, A. C. Pouleur, S. Horman, S. Vaulont, J. Hoerter, B. Viollet, L. Hue, J. L. Vanoverschelde, L. Bertrand, Role of the alpha2-isoform of AMP-activated protein kinase in the metabolic response of the heart to no-flow ischemia. *Am J Physiol* **291**, H2875-2883 (2006).
25. E. Zarrinpashneh, C. Beauloye, A. Ginion, A. C. Pouleur, X. Havaux, L. Hue, B. Viollet, J. L. Vanoverschelde, L. Bertrand, AMPKalpha2 counteracts the development of cardiac hypertrophy induced by isoproterenol. *Biochem Biophys Res Commun* **376**, 677-681 (2008).
26. H. B. Thibault, B. Kurtz, M. J. Raher, R. S. Shaik, A. Waxman, G. Derumeaux, E. F. Halpern, K. D. Bloch, M. Scherrer-Crosbie, Noninvasive assessment of murine pulmonary arterial pressure: validation and application to models of pulmonary hypertension. *Circulation. Cardiovascular imaging* **3**, 157-163 (2010).
27. M. Wang, T. Shibamoto, Y. Kuda, M. Tanida, T. Zhang, J. Song, Y. Kurata, The responses of pulmonary and systemic circulation and airway to anaphylactic mediators in anesthetized BALB/c mice. *Life Sci* **147**, 77-84 (2016).
28. R. S. Baliga, R. J. MacAllister, A. J. Hobbs, New perspectives for the treatment of pulmonary hypertension. *Br J Pharmacol* **163**, 125-140 (2011).

29. S. MacMillan, A. M. Evans, AMPK-alpha1 or AMPK-alpha2 Deletion in Smooth Muscles Does Not Affect the Hypoxic Ventilatory Response or Systemic Arterial Blood Pressure Regulation During Hypoxia. *Front Physiol* **9**, 655 (2018)10.3389/fphys.2018.00655).
30. K. Carvajal, E. Zarrinpashneh, O. Szarszoi, F. Joubert, Y. Athea, P. Mateo, B. Gillet, S. Vaulont, B. Viollet, X. Bigard, L. Bertrand, R. Ventura-Clapier, J. A. Hoerter, Dual cardiac contractile effects of the alpha2-AMPK deletion in low-flow ischemia and reperfusion. *Am J Physiol* **292**, H3136-3147 (2007).
31. M. M. Sung, B. N. Zordoky, A. L. Bujak, J. S. Lally, D. Fung, M. E. Young, S. Horman, E. J. Miller, P. E. Light, B. E. Kemp, G. R. Steinberg, J. R. Dyck, AMPK deficiency in cardiac muscle results in dilated cardiomyopathy in the absence of changes in energy metabolism. *Cardiovasc Res* **107**, 235-245 (2015).
32. K. Sakamoto, A. McCarthy, D. Smith, K. A. Green, D. Grahame Hardie, A. Ashworth, D. R. Alessi, Deficiency of LKB1 in skeletal muscle prevents AMPK activation and glucose uptake during contraction. *EMBO J* **24**, 1810-1820 (2005).
33. K. Sakamoto, E. Zarrinpashneh, G. R. Budas, A. C. Pouleur, A. Dutta, A. R. Prescott, J. L. Vanoverschelde, A. Ashworth, A. Jovanovic, D. R. Alessi, L. Bertrand, Deficiency of LKB1 in heart prevents ischemia-mediated activation of AMPKalpha2 but not AMPKalpha1. *Am J Physiol* **290**, E780-788 (2006).
34. P. Tsou, B. Zheng, C. H. Hsu, A. T. Sasaki, L. C. Cantley, A fluorescent reporter of AMPK activity and cellular energy stress. *Cell Metab* **13**, 476-486 (2011).
35. R. W. Hunter, M. Foretz, L. Bultot, M. D. Fullerton, M. Deak, F. A. Ross, S. A. Hawley, N. Shpiro, B. Viollet, D. Barron, B. E. Kemp, G. R. Steinberg, D. G. Hardie, K. Sakamoto, Mechanism of action of Compound-13: an alpha1-selective small molecule activator of AMPK. *Chem. Biol.* **21**, 866-879 (2014).
36. N. Ikematsu, M. L. Dallas, F. A. Ross, R. W. Lewis, J. N. Rafferty, J. A. David, R. Suman, C. Peers, D. G. Hardie, A. M. Evans, Phosphorylation of the voltage-gated potassium channel Kv2.1 by AMP-activated protein kinase regulates membrane excitability. *PNAS* **108**, 18132-18137 (2011).
37. J. W. Scott, D. G. Norman, S. A. Hawley, L. Kontogiannis, D. G. Hardie, Protein kinase substrate recognition studied using the recombinant catalytic domain of AMP-activated protein kinase and a model substrate. *J. Mol. Biol.* **317**, 309-323 (2002).
38. B. E. Schaffer, R. S. Levin, N. T. Hertz, T. J. Maures, M. L. Schoof, P. E. Hollstein, B. A. Benayoun, M. R. Banko, R. J. Shaw, K. M. Shokat, A. Brunet, Identification of AMPK Phosphorylation Sites Reveals a Network of Proteins Involved in Cell Invasion and Facilitates Large-Scale Substrate Prediction. *Cell Metab* **22**, 907-921 (2015).
39. T. P. Robertson, K. J. Mustard, T. H. Lewis, J. H. Clark, C. N. Wyatt, E. A. Blanco, C. Peers, D. G. Hardie, A. M. Evans, AMP-activated protein kinase and hypoxic pulmonary vasoconstriction. *Eu J Pharmacol* **595**, 39-43 (2008).
40. J. Bain, L. Plater, M. Elliott, N. Shpiro, C. J. Hastie, H. McLauchlan, I. Klevernic, J. S. Arthur, D. R. Alessi, P. Cohen, The selectivity of protein kinase inhibitors: a further update. *Biochem J* **408**, 297-315 (2007).
41. Y. Lv, L. L. Tang, J. K. Wei, X. F. Xu, W. Gu, L. C. Fu, L. Y. Zhang, L. Z. Du, Decreased Kv1.5 expression in intrauterine growth retardation rats with exaggerated pulmonary hypertension. *Am J Physiol* **305**, L856-865 (2013).

42. L. C. Fu, Y. Lv, Y. Zhong, Q. He, X. Liu, L. Z. Du, Tyrosine phosphorylation of Kv1.5 is upregulated in intrauterine growth retardation rats with exaggerated pulmonary hypertension. *Braz J Med Biol Res* **50**, e6237 (2017).
43. P. T. Mungai, G. B. Waypa, A. Jairaman, M. Prakriya, D. Dokic, M. K. Ball, P. T. Schumacker, Hypoxia triggers AMPK activation through reactive oxygen species-mediated activation of calcium release-activated calcium channels. *Mol Cellular Biol* **31**, 3531-3545 (2011).
44. M. Huttemann, B. Kadenbach, L. I. Grossman, Mammalian subunit IV isoforms of cytochrome c oxidase. *Gene* **267**, 111-123 (2001).
45. S. Horvat, C. Beyer, S. Arnold, Effect of hypoxia on the transcription pattern of subunit isoforms and the kinetics of cytochrome c oxidase in cortical astrocytes and cerebellar neurons. *J Neurochem* **99**, 937-951 (2006).
46. K. M. Kocha, K. Reilly, D. S. Porplycia, J. McDonald, T. Snider, C. D. Moyes, Evolution of the oxygen sensitivity of cytochrome c oxidase subunit 4. *Am J Physiol* **308**, R305-320 (2015).
47. R. Fukuda, H. Zhang, J. W. Kim, L. Shimoda, C. V. Dang, G. L. Semenza, HIF-1 regulates cytochrome oxidase subunits to optimize efficiency of respiration in hypoxic cells. *Cell* **129**, 111-122 (2007).
48. S. Aras, O. Pak, N. Sommer, R. Finley, Jr., M. Huttemann, N. Weissmann, L. I. Grossman, Oxygen-dependent expression of cytochrome c oxidase subunit 4-2 gene expression is mediated by transcription factors RBPJ, CXXC5 and CHCHD2. *Nucleic Acids Res* **41**, 2255-2266 (2013).
49. J. C. Ibe, Q. Zhou, T. Chen, H. Tang, J. X. Yuan, J. U. Raj, G. Zhou, Adenosine monophosphate-activated protein kinase is required for pulmonary artery smooth muscle cell survival and the development of hypoxic pulmonary hypertension. *Am J Respir Cell Mol Biol* **49**, 609-618 (2013).
50. D. A. Goncharov, T. V. Kudryashova, H. Ziai, K. Ihida-Stansbury, H. DeLisser, V. P. Krymskaya, R. M. Tuder, S. M. Kawut, E. A. Goncharova, Mammalian target of rapamycin complex 2 (mTORC2) coordinates pulmonary artery smooth muscle cell metabolism, proliferation, and survival in pulmonary arterial hypertension. *Circulation* **129**, 864-874 (2014).
51. J. Omura, K. Satoh, N. Kikuchi, T. Satoh, R. Kurosawa, M. Nogi, T. Otsuki, K. Kozu, K. Numano, K. Suzuki, S. Sunamura, S. Tatebe, T. Aoki, K. Sugimura, S. Miyata, Y. Hoshikawa, Y. Okada, H. Shimokawa, Protective Roles of Endothelial AMP-Activated Protein Kinase Against Hypoxia-Induced Pulmonary Hypertension in Mice. *Circ Res* **119**, 197-209 (2016).
52. J. T. Sylvester, L. A. Shimoda, P. I. Aaronson, J. P. Ward, Hypoxic pulmonary vasoconstriction. *Physiol Rev* **92**, 367-520 (2012).
53. L. Lantier, J. Fentz, R. Mounier, J. Leclerc, J. T. Treebak, C. Pehmoller, N. Sanz, I. Sakakibara, E. Saint-Amand, S. Rimbaud, P. Maire, A. Marette, R. Ventura-Clapier, A. Ferry, J. F. Wojtaszewski, M. Foretz, B. Viollet, AMPK controls exercise endurance, mitochondrial oxidative capacity, and skeletal muscle integrity. *FASEB J* **28**, 3211-3224 (2014).
54. N. El-Bizri, C. Guignabert, L. Wang, A. Cheng, K. Stankunas, C. P. Chang, Y. Mishina, M. Rabinovitch, SM22alpha-targeted deletion of bone morphogenetic protein receptor 1A in mice impairs cardiac and vascular development, and influences organogenesis. *Development* **135**, 2981-2991 (2008).

55. J. Gomez-Arroyo, S. J. Saleem, S. Mizuno, A. A. Syed, H. J. Bogaard, A. Abbate, L. Taraseviciene-Stewart, Y. Sung, D. Kraskauskas, D. Farkas, D. H. Conrad, M. R. Nicolls, N. F. Voelkel, A brief overview of mouse models of pulmonary arterial hypertension: problems and prospects. *Am J Physiol* **302**, L977-991 (2012).
56. S. H. Vitali, G. Hansmann, C. Rose, A. Fernandez-Gonzalez, A. Scheid, S. A. Mitsialis, S. Kourembanas, The Sugen 5416/hypoxia mouse model of pulmonary hypertension revisited: long-term follow-up. *Pulm Circ* **4**, 619-629 (2014).
57. H. W. Cheng, S. Fisch, S. Cheng, M. Bauer, S. Ngoy, Y. Qiu, J. Guan, S. Mishra, C. Mbah, R. Liao, Assessment of right ventricular structure and function in mouse model of pulmonary artery constriction by transthoracic echocardiography. *J Vis Exp*, e51041 (2014).

Funding: A British Heart Foundation Programme Grant (29885 to AME) was the primary source of funding for this study. Initial studies received additional supported by a Wellcome Trust Programme Grant (081195 to AME). Contributions from FAR and DGH were also supported by a Wellcome Trust Investigator Award (204766 to DGH). **Author contributions:** JMS, SL, AT, CM and AME carried out ultrasound experiments and analysis. JMS and AME carried out mitochondrial imaging. JMS and AME carried out electrophysiology and analysis. SL, JMS and AME completed qPCR. FAR and DGH carried out protein phosphorylation and analysis. SM carried out blood pressure measurements. **Competing interests:** The authors declare that they have no competing interests. **Data and materials availability:** All data needed to evaluate the conclusions in the paper are present in the paper or the Supplementary Materials. The authors would like to thank Kei Sakamoto (Nestlé Institute of Health Sciences, Lausanne, Switzerland) for providing additional supplies of the AMPK activator (C13) at a critical time.

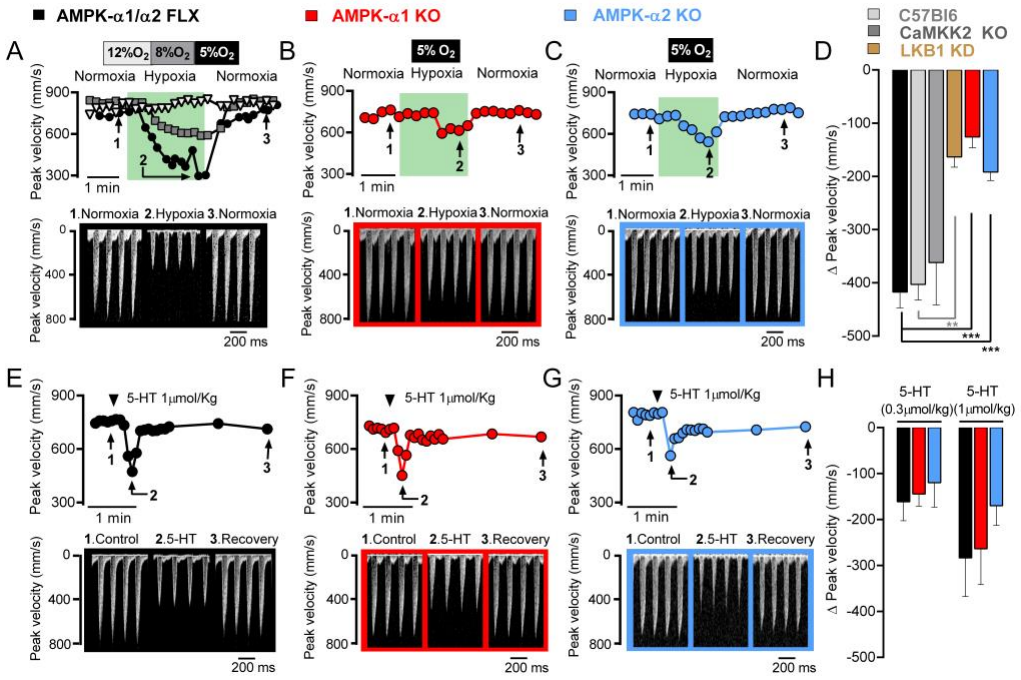

Fig. 1 The LKB1-AMPK but not the CaMKK2-AMPK signalling pathway is required for hypoxic pulmonary vasoconstriction. A-C, Upper panels show spectral Doppler analyses of peak velocity versus time for the systolic waveform within the main pulmonary artery of (A) AMPK-α1 and -α2 floxed controls (AMPK-α1/α2 FLX*)* (B) AMPK-α1 knockout and (C) AMPK-α2 knockout mice during normoxia, hypoxia (12%, 8% or 5% O_2) and recovery. Lower panels show example records of peak velocity during normoxia, hypoxia and recovery. D, Bar chart shows the mean ± SEM for the maximum change in peak velocity observed during 5% O_2 for AMPK-α1/α2 FLX, C57Bl6, CaMKK2 KO, hypomorphic LKB1 floxed (LKB1 KD), AMPK-α1 KO and AMPK-α2 KO mice; n=3-7 mice/group, * P<0.05, ** P<0.01, *** P<0.001. E-G, Upper panels shows spectral Doppler analyses of peak velocity versus time for the systolic waveform within the main pulmonary artery of (E) AMPK-α1 and -α2 floxed controls (AMPK-α1/α2 FLX*)* (F) AMPK-α1 knockout and (G) AMPK-α2 knockout mice during intravenous injection of 5-HT (serotonin). H, Bar chart shows the mean ± SEM for the maximum change in peak velocity observed for AMPK-α1/α2 FLX, AMPK-α1 KO and AMPK-α2 KO mice; n=3-5 mice/group.

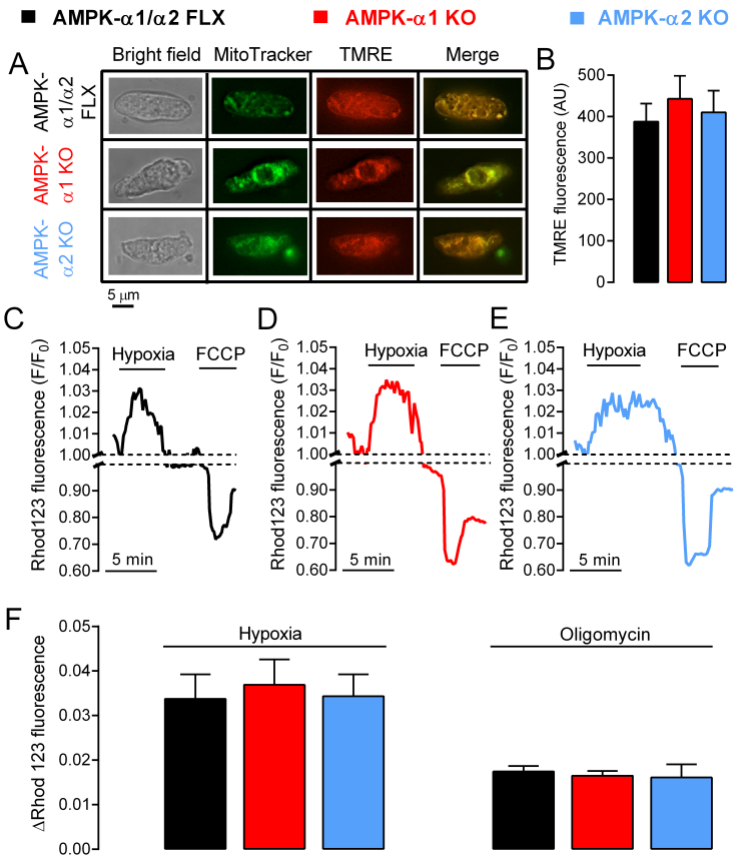

Fig. 2 Deletion of AMPK-α1 or AMPK-α2 does not affect mitochondrial membrane potential. A, Images show a bright-field image of a pulmonary arterial myocyte, deconvolved 3D reconstructions of a Z-stack of images of MitoTracker fluorescence, TMRE fluorescence and a merged image from AMPK-α1/α2 FLX, AMPK-α1 and AMPK-α2 knockout mice. B, Bar chart shows the mean ± SEM for TMRE fluorescence (n=23-34 cells from 4 mice/group). C-E, Records of Rhod123 fluorescence ratio (F/F_0) plotted against time recorded from pulmonary arterial myocytes of (C) AMPK-α1/α2 FLX, (D) AMPK-α1 and (E) AMPK-α2 knockout mice during normoxia and hypoxia. The non-quenching mode was confirmed by adding the mitochondrial uncoupler FCCP (10 µmol/L). F, Bar charts show the mean±SEM for the maximum change in Rhod123 fluorescence during application of hypoxia (~6% O_2) and oligomycin (3 µmol/L). n = 3-6 cells from 3 mice/group.

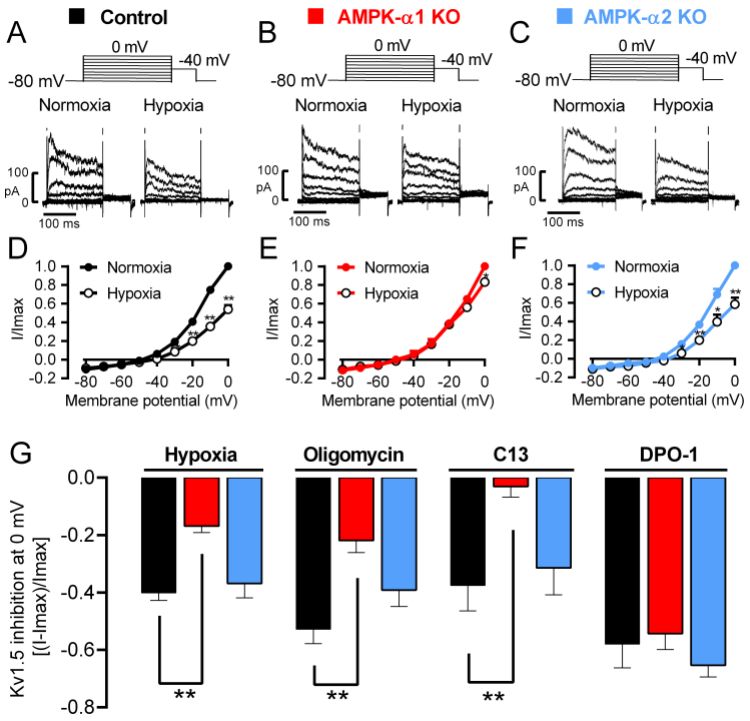

Fig. 3 Deletion of AMPK-α1 but not AMPK-α2 prevents the inhibition of $K_V1.5$ currents by hypoxia and mitochondrial poisons. A-C, Upper panels show the voltage steps applied and example records. Lower panels show raw records of K_V currents activated at each voltage step during normoxia and hypoxia. D-F, Plots (mean ± SEM) for the current-voltage (I/Imax) relationship of steady-state K_V currents recorded (average from last 20 ms of voltage step) during normoxia and hypoxia (≈6% O_2) in acutely isolated pulmonary arterial myocytes from either (D) AMPK-α1/-α2 floxed (control), (E) AMPK-α1 smooth muscle knockout *(*AMPK-α1 KO*)*, or (F) AMPK-α2 smooth muscle knockout (AMPK-α2 KO*)* mice. G, Bar charts show the mean ± SEM for the peak inhibition in K_V current at 0mV (I/I_{max}) for pulmonary arterial myocytes from each genotype during hypoxia and following extracellular application of the mitochondrial poison oligomycin (3 µmol/L), the AMPK-α1 selective agonist C13 (30 µmol/L) and the selective $K_V1.5$ blocker DPO-1 (1 µmol/L); n = 4-9 cells from 3 mice/group; * $P<0.05$, ** $P<0.01$.

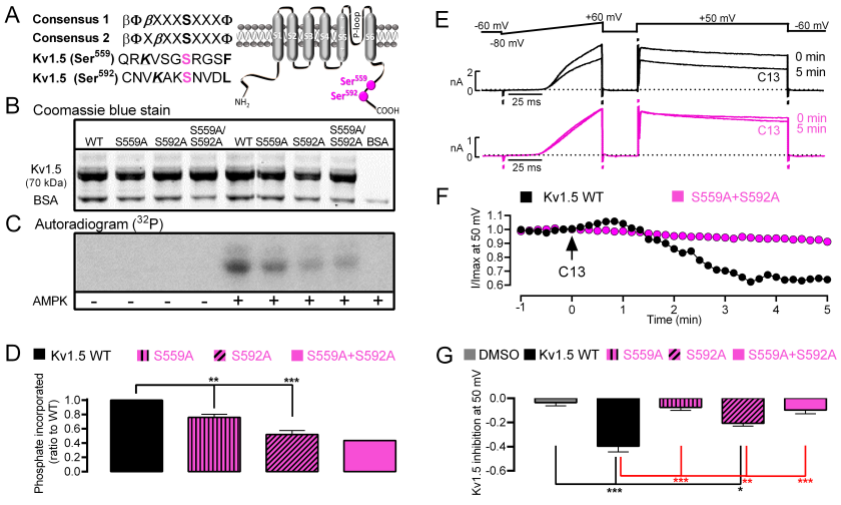

Fig. 4 AMPK inhibits recombinant $K_V1.5$ by direct phosphorylation of two AMPK recognition motifs incorporating Ser^{559} and Ser^{592}. A, Alignment of recognition motif for AMPK with sequences of $K_V1.5$. Phosphorylation sites are marked in pink, β = basic residue, ϕ = hydrophobic residue. Schematic indicates position of residues within $K_V1.5$ α subunit. Coomassie blue stain (B) and autoradiogram (C) show the effect of S559A (n = 3 independent experiments), S592A (n = 3 independent experiments) and S559A/S592A (n = 2 independent experiments) mutations on $K_V1.5$ phosphorylation in cell-free assays by AMPK in the presence of AMP; ** P<0.01, *** P<0.001. D, Fold change in phosphorylation (mutant/wild type) of wild type $K_V1.5$ and $K_V1.5$ mutants incorporating S559A, S592A and S559A/S592A. E, Example records show the effects of C13 on whole-cell K^+ currents, measured by voltage ramp and voltage step protocols, during extracellular application of 30µmol/L C13 in HEK293 cells expressing wild-type $K_V1.5$ and the $K_V1.5$ S559A/S592A mutant. F, Time course for the reductions in whole-cell K^+ currents carried by wild-type and S559A/S592A mutant $K_V1.5$ channels during extracellular application of 30µmol/L C13. G, Bar chart shows the mean ± SEM for reductions in steady-state K^+ currents (average from last 20 ms of voltage step) carried by wild-type and mutant $K_V1.5$ channels 5 min after extracellular application of 30µmol/L C13; n=5-7 cells/group; * P<0.05, *** P<0.001.